Proceedings of the 34th Chinese Control Conference
July 28-30, 2015, Hangzhou, China

Autonomous Landing for Unmanned Seaplanes Based on Active Disturbance Rejection Control

DU Huan[1], FAN Guoliang[1], YI Jianqiang[1]

1. Institute of Automation, Chinese Academy of Sciences, Beijing 100190
E-mail: huan.du@ia.ac.cn

Abstract: Autonomous landing for unmanned seaplanes safely in severe sea states has been a great challenge for decades. A new autonomous landing system of an unmanned seaplane based on active disturbance rejection control (ADRC) is presented in this paper. Firstly, different landing phases of the unmanned seaplane are analyzed. Then according to the characteristics in the different phases, the autonomous landing system consists of a velocity control subsystem and an attitude control subsystem. The velocity control subsystem consists of a velocity ADRC controller and a throttle switch module, while the attitude control subsystem consists of a pitch angle ADRC controller, an altitude PID controller, a pitch angle switch module and a T-S fuzzy reasoning module. Simulations are performed in calm water and irregular wave. The simulations results show that the proposed control system is capable of making the unmanned seaplane land successfully with satisfactory performance.

Key Words: Unmanned seaplane, autonomous landing, active disturbance rejection control

1 Introduction

Unmanned seaplanes, a new type of vehicles that can achieve autonomous takeoff and landing on water, have attracted considerable attention in recent years. Many unmanned seaplanes have been developed, such as Sea Scout, Gull, Flying Fish [1, 2] and so on. Compared with land-based flying vehicles, the typical advantages of unmanned seaplanes are their water movements and water resident operational capability. Hence, they have been widely applied in both military and civilian field, including maritime surveillance, anti-submarine warfare, emergency transportation, ecosystem monitoring and so on [3-5].

For an unmanned aerial vehicle (UAV), landing is the most dangerous stage during a flight. Automatic landing system has been developed to achieve landing on the ground safely for common UAV. Many design approaches were proposed to implement an automatic landing control system, such as PID control [6], LQG/LTR control [7], nonlinear dynamic inversion control [8], intelligent control [9, 10] and so on. However, so far as we know, there is no systematic and comprehensive public literature on landing control system design for unmanned seaplanes except limited studies. The Flying Fish adopted open loop control strategy in the landing stage without considering the effect of sea waves, whose elevator was maintained the maximum [11]. Nebylov developed the technology of landing mode optimization for seaplanes and summarized the optimal landing direction in different wave disturbance, but didn't give related landing system design methods [12].

It is a great challenge to achieve autonomous landing for unmanned seaplanes in high sea states. Firstly, at the moment that the unmanned seaplane contacts on water surface, the hydrodynamic impact is very large. Dynamic instability phenomenon easily occurs if the attitude of the unmanned seaplane is not kept in a proper range, which will lead to the damage of airborne equipment and fuselage structure. Secondly, after landing on water, the wave influences on the unmanned seaplane are so extremely that the unmanned seaplane may jump from wave crest and fall down to wave surface. Therefore, the autonomous landing control system should be able to reduce the hydrodynamic impact with water surface and improve the anti-waves capability of the unmanned seaplane in severe sea states [3].

Active disturbance rejection control (ADRC), inspired by classical PID control, absorbs the results of modern control theory and overcomes some drawbacks of PID [13-15]. The basic idea of ADRC is to regard both internal and external disturbances as an extended system state, and estimate and compensate it using an extended state observer (ESO). Since ADRC does not depend on the accurate system model, it shows good robustness against disturbances and uncertainties. Besides ESO, a typical ADRC consists of other two parts: a tracking differentiator (TD) which is used to arrange transient process and a nonlinear feedback (NF) which is used to construct the feedback control law. ADRC has been successfully applied in many fields in recent years [16-18].

To achieve autonomous landing safely for the unmanned seaplane in severe sea states, a new control scheme is proposed based on ADRC. The proposed control system consists of a velocity control subsystem and an attitude control subsystem. A velocity ADRC controller and a throttle switch module compose the velocity control subsystem, while a pitch angle ADRC controller, an altitude PID controller, a pitch angle switch module and a T-S fuzzy reasoning module compose the attitude control subsystem. This autonomous landing control system is demonstrated to have satisfactory performance by simulation.

The remainder of this paper is organized as follows: Section 2 analyzes the different characteristics in different landing phases and gives related reference commands. An autonomous landing control system is designed based on ADRC in section 3. Section 4 shows the performance of the proposed control system in different wave conditions. Finally, conclusions are obtained in section 5.

*This work is supported by National Natural Science Foundation (NNSF) of China (Grants No. 61273336, 61203003, 61273149, 61421004) and the Innovation Method Fund of China (Grant No. 2012IM010200).

2 Autonomous Landing Analysis of Unmanned Seaplanes

In this section, different phases of autonomous landing of unmanned seaplanes are introduced and related reference commands are given. Firstly, we introduce the nonlinear model of the unmanned seaplane.

2.1 Nonlinear Model of the Unmanned Seaplane

The nonlinear model of the unmanned seaplane presented here is derived by Zhu et al [19] combining fundamental physical laws and empirical methods. Assuming a flat earth and a rigid airframe, the longitudinal dynamics can be described by

$$\left.\begin{aligned} &m\dot{V} = T\cos(\alpha+\alpha_t) - D_a - N_w\sin\alpha - D_f\cdot\cos\alpha + G_{xa} \\ &mV\dot{\alpha} = mVq - T\sin(\alpha+\alpha_t) - L_a - N_w\cdot\cos\alpha + D_f\cdot\sin\alpha + G_{za} \\ &I_y\dot{q} = M_a + M_w + M_T \\ &\dot{\theta} = q \\ &\dot{x}_g = u\cos\theta + w\sin\theta \\ &\dot{z}_g = -u\sin\theta + w\cos\theta \end{aligned}\right\} \quad (1)$$

where V is the velocity, α the angle of attack, q the pitch angular rate, θ the angle of pitch, T the thrust of engine, N_w the water pressure normal to the bottom, D_f the water friction along the bottom, L_a the aerodynamic lift, D_a the aerodynamic drag, G_{xa}, G_{za} the gravity along X_s, Z_s, M_a, M_w, M_T the total pitching moment from air, water and engine, x_g, z_g the position of the unmanned seaplane along X_e, Z_e, u, w the velocity components of the flying boat along X_b, Z_b, I_y the unmanned seaplane's moment of inertia about Y_b, α_t the angle between engine force and X_b, m the mass of the unmanned seaplane.

Fig. 1 shows the forces acting on the unmanned seaplane. Detailed calculation method of the hydrodynamic forces and aerodynamic forces can be found in [19].

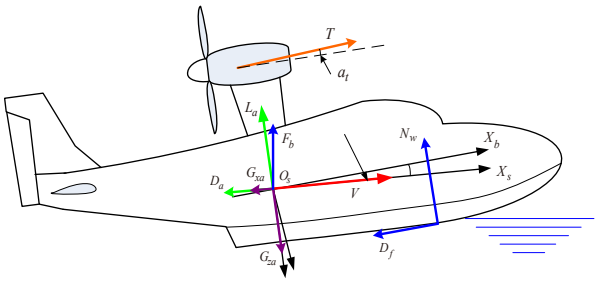

Fig. 1: Forces acting on the unmanned seaplane

2.2 Phases of Autonomous Landing

In this paper, assuming that the unmanned seaplane lands towards the wave propagation direction, only the longitudinal landing system is considered. Total landing process can be divided into approach phase, glide phase, flare phase, falling phase and planing phase, as shown in Fig. 2. Next we mainly introduce the last four phases.

1) Glide phase: The unmanned seaplane descents along the glide path (a certain glide slope) from an altitude of H_2 m. The speed maintains a constant value and the altitude must be controlled in this phase.
2) Flare phase: As the altitude descents to H_1 m, the flare phase begins. The unmanned seaplane flies along a curve trajectory in this phase. In order to make the speed reach a rational range before touching the water surface, the throttle is set to a low level. The speed begins to decrease and the pitch angle gradually increases.
3) Falling phase: As the altitude descents to H_0 m, the unmanned seaplane enters the falling phase. The engine is shut off and the speed continues to decrease. In order to keep a good entry angle with the water surface, the pitch angle must be controlled.
4) Planing phase: In this phase, the unmanned seaplane begins to slide along water surface. When the speed is still fast, the controller should keep the attitude fixed and avoid direct impact with the water surface. When the speed is low, the controller should make the unmanned seaplane track the water surface to reduce the wave impact and ensure the safety.

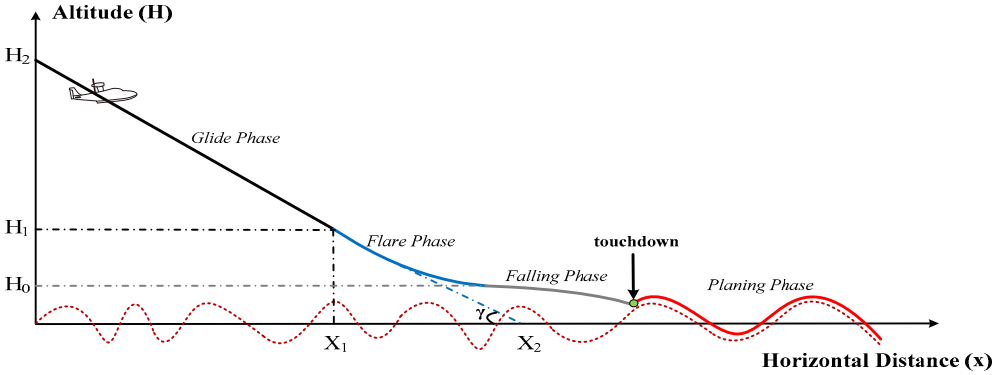

Fig. 2: Different phases of autonomous landing

2.3 Reference Command

According to the above analysis, different control strategy should be adopted in different phases.

Next we give the related reference command in different phases.

1) Glide phase:

The reference altitude command in this phase [20] can be expressed as

$$H_{c1}(x) = (X_2 - x)\tan\gamma \qquad 0 < x \le X_1 \tag{2}$$

where $X_2 = \dfrac{H_2}{\tan\gamma}$, $X_1 = X_2 - \dfrac{H_1}{\tan\gamma}$. X_2 is the crossing point of the sea level and prolongation of the glide path, X_1 is the horizontal position to start the flare phase. H_2 and H_1 is the altitude to start the glide phase and the flare phase, respectively. γ is the flight path angle.

The velocity maintains a constant value, whose reference command can be written as

$$V_c = V_0 \tag{3}$$

2) Flare phase:

The reference altitude command in this phase [20] can be expressed as

$$H_{c2}(x) = H_1 e^{-\frac{x - X_1}{2H_1/\tan\gamma}} \qquad x > X_1 \ and \ H > H_0 \tag{4}$$

where H_0 is the altitude to start the falling phase.

3) Falling phase:

In this phase, a constant pitch angle command is given, which can be written as

$$\theta_c = \theta_0 \tag{5}$$

4) Planing phase:

In order to attain the control object in the planing phase, the reference pitch angle command can be expressed by the following T-S fuzzy reasoning [21]:

$$\begin{aligned} &R_{j,l}: IF \ \ V(t) \ is \ A_j \ and \ h_w(t) \ is \ B_l \ , \\ &THEN \ \ \theta_{j,l} = a_j \cdot (b_{j,l} + w_v(t)) + c_j \cdot \theta_{j,l}^c + k_q \cdot q(t) \end{aligned} \tag{6}$$

where $h_w(t)$ is the relative height to the waves, A_j and B_l are the fuzzy sets corresponding to $V(t)$ and $h_w(t)$, $\theta_{j,l}$ is the reference command, a_j is a parameter to achieve the wave following control for the unmanned seaplane, $b_{j,l}$ is the expected relative angle between the unmanned seaplane and water surface, c_j is a parameter to keep the attitude of the unmanned seaplane in the air, $\theta_{j,l}^c$ is the expected pitch angle, k_q is a parameter to increase the damp of the pitch moments.

The specific calculation and parameter selection of Eq. (6) can be found in [21] and will not be discussed in detail in this paper.

Note that in this paper, we set that $H_2 = 200m$, $H_1 = 20m$, $H_0 = 3m$, $\gamma = 3.5^\circ$, $V_0 = 50m/s$, $\theta_0 = 12^\circ$.

3 Autonomous Landing Control System Design

According to the analysis of different landing phases, an autonomous landing control system is designed based on ADRC for the unmanned seaplane. The control system architecture is shown in Fig. 3. It can be seen that the autonomous landing control system consists of a velocity control subsystem and an attitude control subsystem. The velocity control subsystem consists of a velocity ADRC controller (ADRC L1) and a throttle switch module, while the attitude control subsystem consists of a pitch angle ADRC controller (ADRC L2), an altitude PID controller (PID L3), a pitch angle switch module and a T-S fuzzy reasoning module. Next we design these parts respectively.

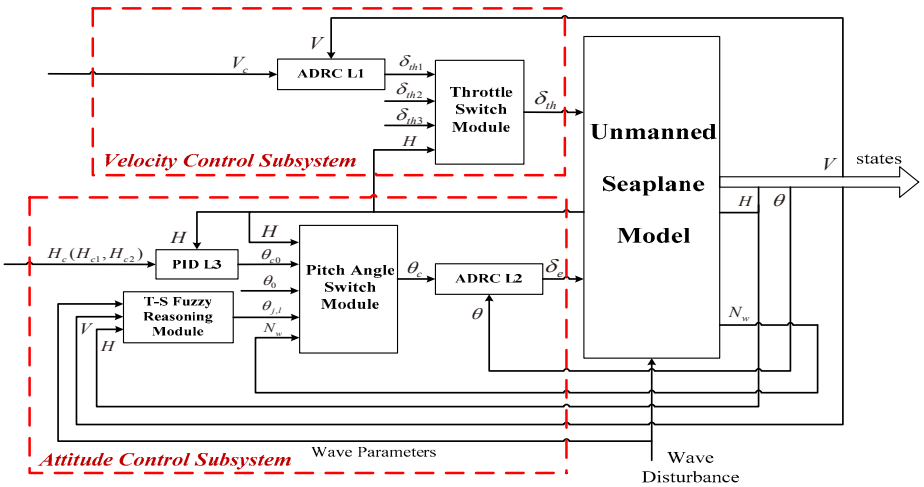

Fig. 3: Autonomous landing control system architecture

3.1 Velocity ADRC Controller Design

Define

$$f_V = \frac{-D_a - N_w \sin\alpha - D_f \cdot \cos\alpha + G_{xa}}{m} \tag{7}$$

$$b_V = \frac{C_T^{\delta_{th}} \cos(\alpha + \alpha_t)}{m} \tag{8}$$

where $C_T^{\delta_{th}}$ is the thrust coefficient.

The first equation of Eq. (1) can be rewritten as

$$\dot{V} = f_V + b_V \delta_{th1} \tag{9}$$

It can be seen from (9) that the throttle-velocity system is of first-order. Therefore, a first-order ADRC controller can be designed.

1) Tracking Differentiator (TD)

The discrete form of TD can be expressed as

$$\begin{cases} v_1(k+1) = v_1(k) + T_s v_2(k) \\ v_2(k+1) = v_2(k) + T_s \cdot fh \\ fh = fhan(v_1(k) - V_c(k), v_2(k), r, h) \end{cases} \tag{10}$$

where $v_1(k)$ tracks the desired velocity $V_c(k)$ and $v_2(k)$ tracks the derivative of $V_c(k)$, T_s is the sampling period. The function *fhan* is the time-optimal solution that guarantees the fastest convergence from v_1 to v without overshoot and its expression can be found in [14]. The parameters r and h are called "speed factor" and "filter factor", which determine the tracking speed and the filtering effect, respectively.

As the velocity ADRC controller is of first-order, only $v_1(k)$ is used in the controller design.

2) Extended State Observer (ESO)

The discrete form of ESO can be expressed as

$$\begin{cases} e(k) = z_1(k) - V(k) \\ z_1(k+1) = z_1(k) + T_s[z_2(k) - \beta_{V01} fal(e(k), \alpha_1, \delta) + b_V \delta_{th1}(k)] \\ z_2(k+1) = z_2(k) - T_s \beta_{V02} fal(e(k), \alpha_2, \delta) \end{cases} \tag{11}$$

where

$$fal(e, \alpha, \delta) = \begin{cases} |e|^{\alpha} \operatorname{sgn}(e), & |e| > \delta, \\ e / \delta^{1-\alpha}, & |e| \le \delta, \end{cases} \quad \delta > 0 \tag{12}$$

Generally, the parameters α_1 and α_2 are set as: $\alpha_1 = 0.5$, $\alpha_2 = 0.25$. If the parameters β_{V01}, β_{V02} and δ are chosen properly, the ESO can well estimate the system states and the total disturbance in real time, that is, $z_1 \to V$, $z_2 \to f_V$.

3) Nonlinear Feedback (NF)

The NF u_0 can be expressed as

$$\begin{cases} e_1 = v_1(k) - z_1(k) \\ u_0 = \beta_{V1} fal(e_1, c_1, \delta_1) \end{cases} \tag{13}$$

Generally, $0 < c_1 < 1$. With the proper parameters β_{V1}, c_1 and δ_1, good control effect can be obtained. The control law is designed as the following form by well compensated for f_V using z_2:

$$\delta_{th1}(k) = u_0 - z_2(k) / b_V \tag{14}$$

3.2 Throttle Switch Module Design

The function of the throttle switch module is to provide the different throttle commands in different landing phases. According to the analysis in section 2, the throttle switch module can be designed as

$$\delta_{th} = \begin{cases} \delta_{th1}, & H > H_1 \\ \delta_{th2}, & H_0 < H \le H_1 \\ \delta_{th3}, & H \le H_0 \end{cases} \tag{15}$$

where δ_{th1} is obtained by Eq. (14), $\delta_{th2} = 0.1 \max(\delta_{th})$, $\delta_{th3} = \min(\delta_{th})$.

3.3 Pitch Angle ADRC Controller Design

Define

$$f_\theta = \frac{M_w + M_T}{I_y} \tag{16}$$

$$b_\theta = \frac{M_a^{\delta_e}}{I_y} \tag{17}$$

where $M_a^{\delta_e}$ is the aerodynamic coefficient.

The third and forth equation of Eq. (1) can be rewritten as

$$\ddot{\theta} = f_\theta + b_\theta \delta_e \tag{18}$$

It can be seen from (17) that the elevator-pitch angle system is of second-order. Therefore, a second-order ADRC controller can be designed.

1) Tracking Differentiator (TD)

The TD here is the same as Eq. (10). $v_1(k)$ and $v_2(k)$ track the desired pitch angle $\theta_c(k)$ and its derivative, respectively.

2) Extended State Observer (ESO)

The discrete form of ESO can be expressed as

$$\begin{cases} e(k) = z_1(k) - \theta(k) \\ z_1(k+1) = z_1(k) + T_s[z_2(k) - \beta_{\theta 01} e(k)] \\ z_2(k+1) = z_2(k) + T_s[z_3(k) - \beta_{\theta 02} fal(e(k), \alpha_1, \delta) + b_\theta \delta_e(k)] \\ z_3(k+1) = z_3(k) - T_s \beta_{\theta 03} fal(e(k), \alpha_2, \delta) \end{cases} \tag{19}$$

If the parameters $\beta_{\theta 01}$, $\beta_{\theta 02}$, $\beta_{\theta 03}$ and δ are chosen properly, the ESO can yield $z_1 \to \theta$, $z_2 \to q$, $z_3 \to f_\theta$.

3) Nonlinear Feedback (NF)

The NF u_0 can be expressed as

$$\begin{cases} e_1 = v_1(k) - z_1(k) \\ e_1 = v_2(k) - z_2(k) \\ u_0 = \beta_{\theta 1} fal(e_1, c_1, \delta_1) + \beta_{\theta 2} fal(e_2, c_2, \delta_1) \end{cases} \tag{20}$$

Generally, $0 < c_1 < 1 < c_2$. Similarly, the control law can be designed as

$$\delta_e(k) = u_0 - z_3(k) / b_\theta \tag{21}$$

3.4 Altitude PID Controller Design

As the outer loop controller, the altitude PID controller is used to generate the desired pitch angle command in the glide phase and flare phase, which can be expressed as

$$\theta_{c0} = k_{hp} e_h + k_{hi} \int e_h dt + k_{hd} \dot{e}_h \tag{22}$$

where $e_h = H_c - H$, k_{hp}, k_{hi}, k_{hd} are the corresponding proportional, integral and differential parameters. H_c can be written as

$$H_c(x) = \begin{cases} H_{c1}(x), & 0 < x \le X_1 \\ H_{c2}(x), & x > X_1 \ and \ H > H_0 \end{cases} \tag{23}$$

3.5 Pitch Angle Switch Module Design

The function of the pitch angle switch module is to provide the different desired pitch angle commands for the ADRC controller in different landing phases. According to the analysis in section 2, the pitch angle switch module can be designed as

$$\theta_c = \begin{cases} \theta_{c0}, & H > H_0 \\ \theta_0, & H \le H_0 \ and \ N_w = 0 \\ \theta_{j,l}, & N_w \ne 0 \end{cases} \tag{24}$$

where N_w is the hydrodynamic force, θ_{c0} is obtained by Eq. (21) and θ_0, $\theta_{j,l}$ have been given in section 2.

The T-S fuzzy reasoning module has been discussed in section 2 and will not be given in this section.

The above parts compose the total autonomous landing control system. Due to the robustness of ADRC controller, the control system can improve the sea-keeping ability of the unmanned seaplane effectively.

4 Simulation Results

In this section, an unmanned seaplane model with a height of 1.09m is used to demonstrate the performance of the autonomous landing control system. Two different wave conditions are provided in the simulation: calm water and irregular wave. The initial trimmed states of the unmanned seaplane are chosen as: $V = 50m/s$, $\alpha = -1.97^\circ$, $q = 0rad/s$, $\theta = -1.97^\circ$, $H = 200m$.

Firstly, Fig.6 and Fig.7 present the autonomous landing performance of the unmanned seaplane in calm water. It can be seen from Fig. 6 that in the glide phase (before about 60s), the unmanned seaplane tracks the reference trajectory closely. Figs. 7 (a) and (b) show that the velocity and the pitch angle are controlled in a constant value. The unmanned seaplane turns into the flare phase at about 60s. As the throttle is set in a low level as shown in Fig. 7 (e), the velocity begins to decrease and the pitch angle begins to increase. The trajectory tracking still has a good effect in this phase as shown in the enlarged portion of Fig. 6. In order to keep a good entry angle with the water surface, the pitch angle is controlled in a larger value in the falling phase (about 76s~83s), at the same time, the throttle has been set to zero. The height increases slightly in this phase with the increase of the pitch angle as shown in the enlarged portion of Fig. 6. At about 83s, the unmanned seaplane begins to land on water. Fig. 7 (d) show that the hydrodynamic impact is large at this moment, while the large variability for the pitch angular rate and the elevator deflection can be seen in Figs. 7 (c) and (f). After landing on water, the hydrodynamic force decreases gradually and the states of the unmanned seaplane become to be stable.

Secondly, the simulation is performed in irregular wave, which is equivalent to Seastate 3 and the significant wave height exceeds one meter [22]. As the distance between the center of gravity and the bottom is only 0.552m for the unmanned seaplane, this irregular wave belongs to the severe sea state. The state changes in the first three phases in irregular wave are identical to the ones in calm water as shown in Fig. 8 and Fig. 9. However, Figs. 9 (b) (c) (d) show that the hydrodynamic force is very large just after touchdown so that the pitch angle and the pitch angular rate fluctuate in a large range. In the meanwhile, there appears the elevator saturation as shown in Fig. 9 (f). Since this irregular wave is huge for the unmanned seaplane, this is acceptable. The enlarged portion of Fig. 8 shows that after landing, the unmanned seaplane can follow the water surface well, reducing the water impacts. The unmanned seaplane can achieve autonomous landing safely via the proposed controller in the severe sea states.

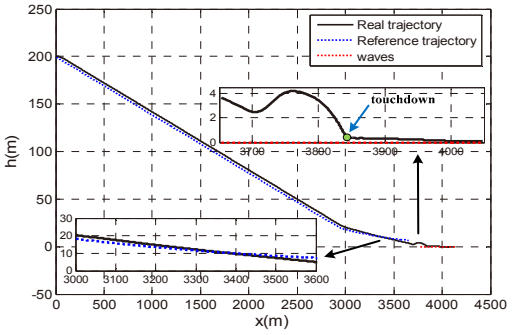

Fig. 6: Landing trajectory in calm water

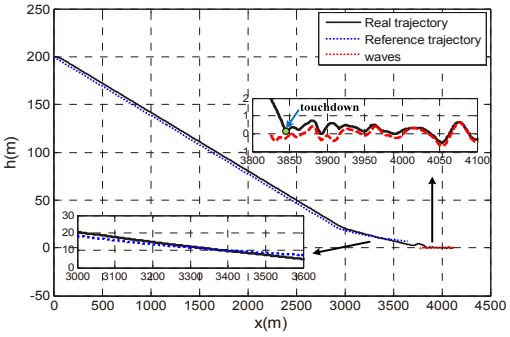

Fig. 8: Landing trajectory in irregular wave

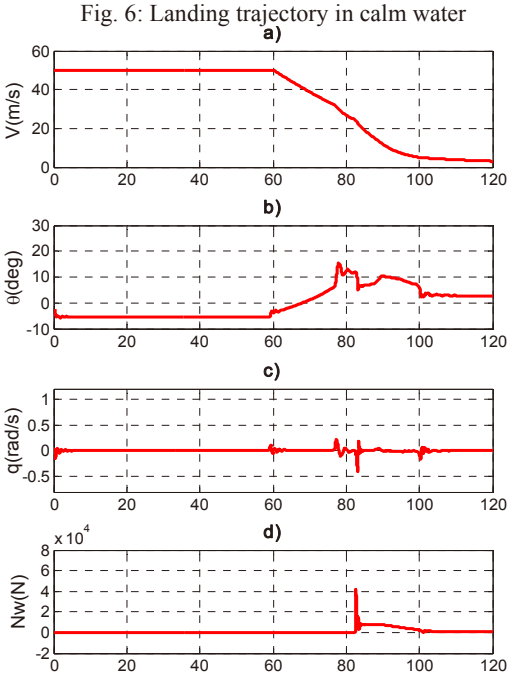

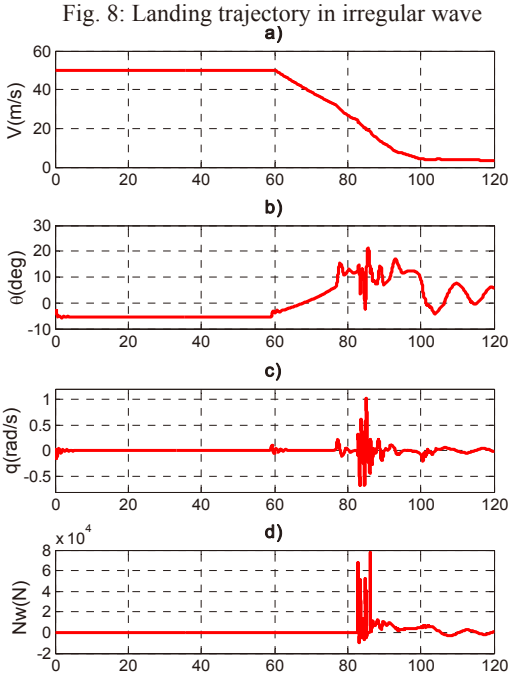

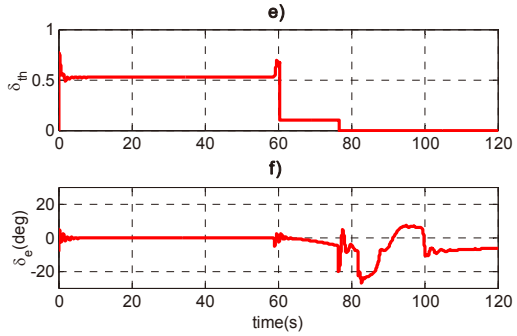

Fig. 7: Performance of the unmanned seaplane in clam water

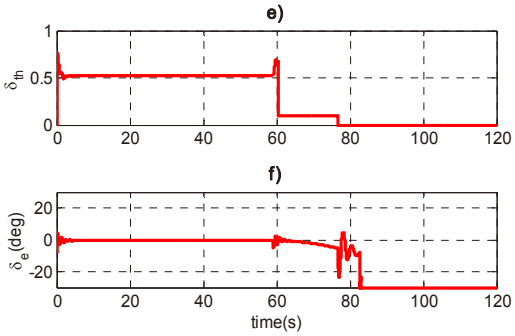

Fig. 9: Performance of the unmanned seaplane in irregular wave

5 Conclusion

In this paper, a new autonomous landing control system for an unmanned seaplane is presented, aiming to ensure the safety and improve the anti-waves capability in high sea states. According to the analysis in different landing phases, this control system is designed based on ADRC. The proposed control system is composed of a velocity control subsystem and an attitude control subsystem. The velocity control subsystem is composed of a velocity ADRC controller and a throttle switch module, while the attitude control subsystem is composed of a pitch angle ADRC controller, an altitude PID controller, a pitch angle switch module and a T-S fuzzy reasoning module. The simulation results show that the proposed control system has satisfactory performance in different sea states, improving the sea-keeping ability of the unmanned seaplane.

References

[1] R. D. Eubank, and E. M. Atkins, Unattended autonomous mission and system management of an unmanned seaplane, in *Proceedings of Infotech@Aerospace*, 2011, AIAA 2011-1614.

[2] G. Meadows, E. Atkins, P. Washabaugh, L. Meadows, L. Bernal, B. Gilchrist, D. Smith, H. VanSumeren, D. Macy, R. Eubank, B. Smith, and J. Brown, The Flying Fish persistent ocean surveillance platform, in *Proceedings of AIAA Infotech@Aerospace Conference*, 2009, AIAA 2009-1902.

[3] H. Du, G. Fan, and J. Yi, Autonomous takeoff control system design for unmanned seaplanes, *Ocean Engineering*, 85: 21-31, 2014.

[4] X. Yang, T. Wang, J. Liang, G. Yao, and M. Liu, Survey on the novel hybrid aquatic-aerial amphibious aircraft: Aquatic unmanned aerial vehicle (AquaUAV), *Progress in Aerospace Sciences*, Article in Press.

[5] L. Chu, and S. Ye, *Collected Works of Seaplane*. Beijing: Aviation Industry Press, 2011.

[6] F.-B. Hsiao, W.-L. Chan, Y.-C. Lai, L.-C. Tseng, S.-Y. Hsieh, and H.-K. Tenn, Landing longitudinal control system design for a fixed wing UAV, in *Proceedings of 45th AIAA Aerospace Sciences Meeting and Exhibit*, 2007, AIAA 2007-868.

[7] A. Alonge, F. D. Ippolito, and C. Grillo, Takeoff and landing robust control system for a tandem canard UAV, in *Proceedings of AIAA/CIRA 13th International Space Planes and Hypersonics Systems and Technologies*, 2005, AIAA 2005-3447.

[8] R. Lungu, M. Lungu, and L. T. Grigorie, Automatic control of aircraft in longitudinal plane during landing, *IEEE Transactions on Aerospace and Electronic Systems*, 49(2): 1338-1350, 2013.

[9] K. Nho, and R. K. Agarwal, Automatic landing system design using fuzzy logic, *Journal of Guidance, Control, and Dynamics*, 23(2): 298-304, 2000.

[10] J.-G. Juang, and K.-C. Cheng, Application of neural networks to disturbances encountered landing control, *IEEE Transactions on Intelligent Transportation Systems*, 7(4): 582-588, 2006.

[11] R. D. Eubank, and E. M. Atkins, Autonomous guidance and control of the flying fish ocean surveillance platform, in *Proceedings of AIAA Infotech@Aerospace Conference*, 2009, AIAA 2009-2021.

[12] V. Nebylov, and A. Nebylov, Seaplane landing smart control at wave disturbances, in *Proceedings of 18th IFAC World Congress*, 2011: 3021-3026.

[13] J. Han, From PID to active disturbance rejection control, *IEEE Transactions on Industrial Eletronics*, 56(3): 900-906, 2009.

[14] J. Han, *Active Disturbance Rejection Control Technique — The Technique for Estimating and Compensating the Uncertainties*. Beijing: National Defence Industry Press, 2008.

[15] B. Guo, and Z. Zhao, On convergence of the nonlinear active disturbance rejection control for MIMO systems, *SIAM Journal on Control and Optimization*, 51(2): 1727-1757, 2013.

[16] B. Sun, and Z. Gao, A DSP-based active disturbance rejection control design for a 1-kW H-bridge DC-DC power converter, *IEEE Transactions on Industrial Eletronics*, 52(5): 1271-1277, 2005.

[17] Q. Zheng, L. Dong, D. H. Lee, and Z. Gao, Active disturbance rejection control for MEMS gyroscopes, *IEEE Transactions on Control Systems Technology*, 17(6): 1432-1438, 2009.

[18] Y. Huang, K. Xu, J. Han, and J. Lam, Flight control design using extended state observer and non-smooth feedback, in *Proceedings of 40th IEEE Conference on Decision and Control*, 2001: 223-228.

[19] Y. Zhu, G. Fan, and J. Yi, Modeling for flying boats in regular wave, in *Proceedings of 10th World Congress on Intelligent Control and Automation*, 2012: 3019-3024.

[20] H. Xiong, J. Yi, G. Fan, and F. Jing, Anti-crosswind autolanding of UAVs based on active disturbance rejection control, in *Proceedings of AIAA Guidance, Navigation, and Control Conference*, 2010, AIAA 2010-7734.

[21] Y. Zhu, G. Fan, and J. Yi, Controller design based on T-S fuzzy reasoning and ADRC for a flying boat, in *Proceedings of 10th IEEE International Conference on Control and Automation*, 2013: 1578-1583.

[22] T. I. Fossen, *Guidance and Control of Ocean Vehicles*. New York: John Wiley & Sons, 1994.